Published in final edited form as:
Nature. 2010 June 17; 465(7300): 927–931. doi:10.1038/nature09079.

Fine-Tuning of Pre-Balanced Excitation and Inhibition During Auditory Cortical Development

Yujiao J. Sun[1], **Guangying K. Wu**[1], **Bao-hua Liu**[1], **Pingyang Li**[1], **Mu Zhou**[1], **Zhongju Xiao**[4], **Huizhong W. Tao**[1,3,*], and **Li I. Zhang**[1,2,*]

[1]Zilkha Neurogenetic Institute, Keck School of Medicine, University of Southern California, Los Angeles, CA 90089, USA

[2]Department of Biophysics and Physiology, Keck School of Medicine, University of Southern California, Los Angeles, CA 90089, USA

[3]Department of Cell and Neurobiology, Keck School of Medicine, University of Southern California, Los Angeles, CA 90089, USA

[4]Department of Physiology, School of Basic Medical Sciences, Southern Medical University, Guangzhou 510515, China

Abstract

Functional receptive fields of neurons in sensory cortices undergo progressive refinement during development[1-4]. Such refinement may be attributed to the pruning of non-optimal excitatory inputs, reshaping of the excitatory tuning profile through modifying the strengths of individual inputs, or strengthening of cortical inhibition. These models have not been directly tested, due to the technical difficulties in assaying the spatiotemporal patterns of functional synaptic inputs during development. In this study, *in vivo* whole-cell voltage-clamp recordings were applied to the recipient layer 4 neurons in the rat primary auditory cortex (A1) to determine the developmental changes in the frequency-intensity tonal receptive fields (TRFs) of their excitatory and inhibitory inputs. To our surprise, co-tuned excitation and inhibition were observed right after the onset of hearing, suggesting that a tripartite thalamocortical circuit with relative strong feedforward inhibition is formed independent of auditory experience. The frequency ranges of tone-driven excitatory and inhibitory inputs first expand within a few days after the hearing onset and then persist into adulthood. The latter phase is accompanied by a sharpening of the excitatory but not inhibitory frequency tuning profile, which results in a relatively broader inhibitory tuning in adult A1 neurons. Thus, the development of cortical synaptic TRFs after hearing onset is marked by a slight breakdown of priorly formed excitation-inhibition balance. Our results suggest that functional refinement of cortical TRFs does not require a selective pruning of inputs, but may depend more on a fine adjustment of excitatory input strengths.

To account for the refinement of spike receptive fields (i.e. RFs of spiking/suprathreshold responses) in sensory cortices during postnatal development, three synaptic mechanisms can be proposed (Fig. 1a). First, selective pruning of excitatory inputs at RF peripheries reduces the total range of inputs. Second, modifying the strengths of individual inputs, e.g. weakening the inputs at RF peripheries, can effectively reduce the size of the spike RF without changing the total input range. Third, broadening of the inhibitory tuning and/or strengthening of inhibition can also effectively reduce the spike RF size. However, these models could not be

* Correspondence should be addressed to: L.I.Z. (liizhang@usc.edu) or H.W.T. (htao@usc.edu).

Author Contributionons: Y.J.S., G.K.W., P.L. and M.Z. performed the experiments. Y.J.S., B.-h.L. and Z.X. carried out the data analysis. H.W.T. and L.I.Z. designed the experiments and analysis, and wrote the manuscript.

directly revealed by previous anatomical, extracellular recording or cortical slice studies. It is also worth noting that although inhibition is proposed to play an important role in regulating the critical period for cortical plasticity[5], how the inhibitory circuits undergo developmental changes has not been well elucidated. In this study, we intended to address these issues in the rat A1, the functional development of which is marked by a progressive refinement of the tonotopic map and sharpening of spike TRFs of neurons[3,6]. Synaptic TRFs in the recipient layer 4 of the adult A1 are characterized by approximately balanced excitation and inhibition as well as a stereotypic temporal delay of inhibition relative to excitation[7-10], which can be attributed to a tripartite thalamocortical feedforward circuit[9,11, 12].

To examine the developmental changes in synaptic TRFs, whole-cell voltage-clamp recordings were made from layer 4 neurons of rats at different ages. Brief tones of various frequencies and intensities were applied to map TRFs (see Methods). Excitatory responses were recorded at -80mV, while inhibitory responses at 0mV. As shown in Fig. 1b, these synaptic inputs could be reasonably clamped. We first examined whether there was an initial mismatch between excitatory and inhibitory TRFs in early development, as suggested by a study in the developing *Xenopus* retinotectal system[13]. At postnatal day 12-13 (P12-P13), the ear canals are just opened and auditory responses can first be detected in the A1[3,6]. Surprisingly, at this stage right after the hearing onset, excitatory and inhibitory TRFs already appeared well matched in the frequency-intensity space (Fig. 1c). The intensity thresholds for evoking excitatory and inhibitory responses were both notably high, mostly at or above 70dB sound pressure level (SPL). Comparison of excitatory and inhibitory tuning curves (i.e. the envelope of peak response amplitudes) revealed that they did not match well at the threshold intensity (Fig. 1d, 70dB). However, at intensities above the threshold, they did match reasonably well in terms of frequency range and shape (Fig. 1d, 90dB; Supplementary Fig. 1), similar as reported in the adult A1[7-9].

To quantify the degree of mismatch between the excitatory and inhibitory tuning curves, we used a mismatch index (MMI; see Methods). For a group of P12-P14 neurons, MMI value was in general high for synaptic tuning curves at threshold intensity (Fig. 1e). This, however, should not be simply interpreted as poorly matched excitatory and inhibitory tunings, but rather can be attributed to the unreliability of synaptic responses at the threshold and the limited number of sampling trials. In fact, similarly high MMI values at threshold intensity were also observed for adult neurons (Fig. 1e). This argues for the necessity of examining excitation-inhibition balance at intensity levels above threshold. Indeed, at higher intensities, P12-P13 neurons exhibited low MMI values comparable to adult neurons (Fig. 1e), indicating that the excitation-inhibition balance as observed in the adult A1 is already established at stages right after the hearing onset. Given that the intensity threshold for auditory nerve-brainstem evoked response (ABR) at P12-P13 is similarly high as the cortical response (70 -100 dB)[14,15], the cortex and subcortical nuclei may not be effectively driven under usual auditory environment at stages around the hearing onset. Therefore the establishment of excitation-inhibition balance is likely independent of auditory experience, reminiscent of the formation of ocular dominance columns and orientation maps in the developing visual cortex which is visual experience-independent[16,17]. These observations also support the previous hypothesis that at or even before the hearing onset, the hard wiring is already present between auditory nuclei in the ascending pathway[18].

We next examined older stages. Compared to P12-P13, the intensity threshold for synaptic responses at P16 drastically reduced and the frequency-intensity area for synaptic responses markedly expanded (Fig. 2a). The intensity threshold did not appear to further decrease after P16 (Fig. 2b-c). For all the neurons, excitatory and inhibitory synaptic TRFs appeared largely matched (Fig. 2a-c). Comparing the synaptic tuning curves at the same relative intensity level (Fig. 2d), we did not observe appreciable developmental changes in the total frequency

responding range of synaptic inputs (TFRR; see Methods). However, the shape of the excitatory tuning curve in relation to that the inhibitory tuning curve appeared quite different between P16 and P80. At P16, the excitatory and inhibitory tuning curves both exhibited a broad peak, and they matched exquisitely. At P80, the peak of the excitatory tuning curve appeared much sharpened, while that of the inhibitory tuning curve remained broad (Fig. 2d, Supplementary Fig.1). Thus, the excitatory and inhibitory tuning curves at P80 appeared less matched. This observation of a slight mismatch between excitatory and inhibitory tunings is consistent with our previous report[10], which shows that a relatively broader inhibitory tuning can generate an equivalent lateral inhibitory sharpening effect.

To summarize the developmental changes in synaptic TRFs, neurons were grouped into four developmental stages: stage 1 (ST1), from P12 to P14; ST2, from P15 to P18; ST3, from P19 to P25; and ST4, P80 and older. There was a rapid decrease in intensity threshold from ST1 to ST2 for both excitatory and inhibitory TRFs (Fig. 3a). The intensity threshold of the inhibitory TRF was mostly the same as that of the excitatory TRF. Only in a small fraction of neurons, it was slightly (≤10 dB) higher. In parallel, the intensity threshold of spike TRFs, as examined by cell-attached recordings (see Methods), became lowered with development (Fig. 3a), which is consistent with previous results3،6. This change in intensity threshold is likely attributed to the functional maturation of the periphery, since the intensity threshold for ABR decreases from 70-100 dB at P12-13 to 30-50 DB at P16 (ref 14،15). The ranges of excitatory and inhibitory inputs became enlarged from ST1 to ST2, as shown by the TFRRs at 10 dB above threshold (Fig. 3b). The TFRRs did not further change after ST2 (Fig. 3b). The bandwidth of the excitatory tuning curve at the level of 50% of the peak (BW50%) initially increased from ST1 to ST2 (Fig. 3c), consistent with the change in TFRR. However, after ST2, it significantly decreased, indicating that the shape of the excitatory tuning curve is sharpened without reducing the total range of inputs. In contrast, BW50% of the inhibitory tuning curve remained stable after ST2 (Fig. 3c), indicating that the inhibitory tuning does not undergo a significant developmental sharpening. The differential development of excitatory and inhibitory tunings leads to a slight breakdown of the priorly formed excitation-inhibition balance, as indicated by a significantly higher MMI at ST4 than at ST2 (Fig. 3d). At more mature stages, the relatively broader inhibitory tuning was observed for neurons exhibiting various characteristic frequencies (CF) (Supplementary Fig. 2). It is worth noting that despite the slight mismatch, excitation and inhibition are by and large in balance, as indicated by the strong correlation between their amplitudes (Supplementary Fig. 3).

We noted that in another study, Dorrn et al. found that the developmental establishment of balanced excitation and inhibition in the auditory cortex was a protracted process, with a relatively low level of co-tuning shortly after the hearing onset. This apparently opposite observation may be attributed to several differences in their experimental designs. First, while our study focused on the thalamocortical circuit in layer 4, their recorded neurons spanned layer 3 to 6 and exhibited surprisingly broad frequency ranges of synaptic inputs cross all stages, apparently exceeding their 0.5-32 kHz testing range. Second, they chose a fixed intensity (70 dB) for examining the co-tuning of excitation and inhibition. The synaptic tuning/co-tuning may vary with the intensity level relative to the threshold of synaptic TRFs, which decreases during development. Nevertheless, both studies demonstrated that shortly after the hearing onset, excitation and inhibition with similar amplitudes and temporal relationship as in adults have already engaged in auditory-evoked responses.

We did not observe significant developmental changes in the ratio between the peak amplitudes of inhibition and excitation (I/E ratio) evoked by tones of preferred frequency, or in their absolute amplitudes (Fig. 3e). The onset latencies of excitatory and inhibitory responses become shorter with age, whereas the relative delay of inhibition to the onset of excitation

(about 2ms) remains more or less constant across different stages (Fig. 3f), further suggesting that the tripartite thalamocortical feedforward circuit is already formed at the onset of hearing.

The above data suggest that instead of a selective pruning of inputs at RF peripheries, adjusting the strengths and tuning pattern of excitatory inputs may be a major mechanism for the functional refinement of cortical TRFs. To further understand the impacts of the observed synaptic changes on spike receptive fields, we derived spike TRFs of the recorded neurons by integrating the experimentally determined excitatory and inhibitory synaptic conductances in an integrate-and-fire model (see Methods). To estimate the accuracy of our method of deriving spike TRFs, we carried out sequential cell-attached recording and whole-cell voltage-clamp recording to obtain the *bona fide* spike TRF and synaptic conductances from the same cell. As shown in one example (Fig. 4a), the spike TRF derived from the synaptic conductances was largely consistent with the recorded spike TRF. For five experiments, the percentage deviation of the bandwidth of the derived spike TRF at 10dB above threshold from that of the recorded spike TRF was 3.7% ± 10.0% (mean ± s.d.), suggesting that in these recorded cells the integration of synaptic inputs based on their spectrotemporal interactions could provide a reasonable estimation of the spike output. The summary of bandwidths of the derived spike TRFs shows that spike TRFs are first broadened from ST1 to ST2, and then refined afterwards (Fig. 4b). Furthermore, spike TRFs as examined by cell-attached recordings displayed the same developmental trend (Fig. 4b). These results are consistent with the previous extracellular recording studies[3,6,19], indicating that the observed changes in the patterns of excitatory and inhibitory inputs can largely explain the developmental refinement of spike TRFs.

The developmental changes in the frequency responding ranges and tuning profiles suggest two phases of auditory cortical development: an initial expansion of the synaptic TRFs, and a later modification of the synaptic tuning profiles. The refinement of auditory spike TRFs is mainly contributed by two factors (Fig. 4c). First, instead of the generally proposed reduction of the input range, modulation of the strengths of existing excitatory inputs leads to a sharpening of the excitatory tuning profile. Second, the relatively stable inhibitory tuning compared to the excitatory tuning results in a slight breakdown of the prior excitation-inhibition balance, allowing a lateral inhibitory sharpening effect on the spike TRF at more mature stages[10]. Thus, the modulation of excitatory connections primarily guides the functional development of the auditory cortex, resulting in sharply tuned frequency selectivity and a more distinctive frequency gradient in the tonotopic map.

Methods summary

All experimental procedures used in this study were approved under USC/IACUC. Sprague-Dawley rats from P12 to 3 months old were anaesthetized with ketamine/xylazine. Extracellular multiunit recordings were used to locate the rat A1[7,9,10]. In vivo whole-cell voltage-clamp recordings were applied as previously described[7-10, 20-23]. Excitatory and inhibitory synaptic currents were separated by clamping the cell's membrane potential at -80 mV and 0 mV respectively. The pipette (4-7 MΩ) contained intracellular solution (in mM): 125 Cs-gluconate, 5 TEA-Cl, 2 CsCl, 1 EGTA, 10 HEPES, 4 MgATP, 0.3 GTP, 10 phosphocreatine, 1.5 QX-314, pH 7.2. Cell-attached loose-patch recordings[9,10,23-25] (with pipette containing ACSF) were used to detect spike responses of the recorded neuron. The study focused on excitatory pyramidal neurons in the recipient layer 4 (Ref, 26,27). Pure tones (0.5–64 kHz at 0.1 octave intervals, 25-ms duration, 3ms ramp, a total of 568 testing stimuli) at eight sound intensities (from 0-70 dB SPL except for P12-P14 rats for which 20-90dB were applied) were delivered through a calibrated free-field speaker. Frequency-intensity receptive fields (TRFs) of tone-evoked synaptic and spike responses were reconstructed, and frequency tuning curves of excitatory and inhibitory responses were derived for each testing intensity. As previously described, we computed the excitatory and inhibitory conductances[7-10,22,

23,25,28,29, as well as the derived membrane potential response[8,22,23,25,30] for the recorded neurons.

Supplementary Material

Refer to Web version on PubMed Central for supplementary material.

Acknowledgments

This work was supported by grants to L.I.Z. from the US National Institutes of Health/National Institute on Deafness and Other Communication Disorders (R01DC008983, R21DC008588), the Searle Scholar Program, the Klingenstein Foundation, and the David and Lucile Packard Foundation (Packard Fellowships for Science and Engineering). H.W.T. is supported by the US National Institutes of Health (EY018718 and EY019049) and The Karl Kirchgessner Foundation. Z.X. is supported by National Natural Science Foundation of China (Grant Nos. 30730039, 30970982, and 30670665).

References

1. Katz LC, Shatz CJ. Synaptic activity and the construction of cortical circuits. Science 1996;274:1133–8. [PubMed: 8895456]
2. Fagiolini M, Pizzorusso T, Berardi N, Domenici L, Maffei L. Functional postnatal development of the rat primary visual cortex and the role of visual experience: dark rearing and monocular deprivation. Vision Res 1994;34:709–20. [PubMed: 8160387]
3. Zhang LI, Bao S, Merzenich MM. Persistent and specific influences of early acoustic environments on primary auditory cortex. Nat Neurosci 2001;4:1123–30. [PubMed: 11687817]
4. Inan M, Crair MC. Development of cortical maps: perspectives from the barrel cortex. Neuroscientist 2007;13:49–61. [PubMed: 17229975]
5. Hensch TK. Critical period plasticity in local cortical circuits. Nat Rev Neurosci 2005;6:877–88. [PubMed: 16261181]
6. Chang EF, Merzenich MM. Environmental noise retards auditory cortical development. Science 2003;300:498–502. [PubMed: 12702879]
7. Zhang LI, Tan AY, Schreiner CE, Merzenich MM. Topography and synaptic shaping of direction selectivity in primary auditory cortex. Nature 2003;424:201–205. [PubMed: 12853959]
8. Wehr M, Zador AM. Balanced inhibition underlies tuning and sharpens spike timing in auditory cortex. Nature 2003;426:442–446. [PubMed: 14647382]
9. Tan AY, Zhang LI, Merzenich MM, Schreiner CE. Tone-evoked excitatory and inhibitory synaptic conductances of primary auditory cortex neurons. J Neurophysiol 2004;92:630–43. [PubMed: 14999047]
10. Wu GK, Arbuckle R, Liu BH, Tao HW, Zhang LI. Lateral sharpening of cortical frequency tuning by approximately balanced inhibition. Neuron 2008;58:132–143. [PubMed: 18400169]
11. Douglas RJ, Martin KA. A functional microcircuit for cat visual cortex. J Physiol 1991;440:735–769. [PubMed: 1666655]
12. Oswald AM, Schiff ML, Reyes AD. Synaptic mechanisms underlying auditory processing. Curr Opin Neurobiol 2006;16:371–6. [PubMed: 16842988]
13. Tao HW, Poo MM. Activity-dependent matching of excitatory and inhibitory inputs during refinement of visual receptive fields. Neuron 2005;45:829–36. [PubMed: 15797545]
14. Blatchley BJ, Cooper WA, Coleman JR. Development of auditory brainstem response to tone pip stimuli in the rat. Brain Res 1987;429:75–84. [PubMed: 3567661]
15. Geal-Dor M, Freeman S, Li G, Sohmer H. Development of hearing in neonatal rats: air and bone conducted ABR thresholds. Hear Res 1993;69:236–42. [PubMed: 8226345]
16. Chapman B, Stryker MP, Bonhoeffer T. Development of orientation preference maps in ferret primary visual cortex. J Neurosci 1996;16:6443–6453. [PubMed: 8815923]
17. Katz LC, Crowley JC. Development of cortical circuits: lessons from ocular dominance columns. Nat Rev Neurosci 2002;3:34–42. [PubMed: 11823803]

18. Romand R. Modification of tonotopic representation in the auditory system during development. Prog Neurobiol 1997;51:1–17. [PubMed: 9044426]
19. de Villers-Sidani E, Chang EF, Bao S, Merzenich MM. Critical period window for spectral tuning defined in the primary auditory cortex (A1) in the rat. J Neurosci 2007;27:180–9. [PubMed: 17202485]
20. Moore CI, Nelson SB, Sur M. Dynamics of neuronal processing in rat somatosensory cortex. Trends Neurosci 1999;22:513–520. [PubMed: 10529819]
21. Margrie TW, Brecht M, Sakmann B. In vivo, low-resistance, whole-cell recordings from neurons in the anaesthetized and awake mammalian brain. Pflugers Arch 2002;444:491–498. [PubMed: 12136268]
22. Liu BH, Wu GK, Arbuckle R, Tao HW, Zhang LI. Defining cortical frequency tuning with recurrent excitatory circuitry. Nat Neurosci 2007;10:1594–1600. [PubMed: 17994013]
23. Zhou Y, et al. Preceding inhibition silences layer 6 neurons in auditory cortex. Neuron 2010;65:706–17. [PubMed: 20223205]
24. Liu BH, et al. Visual receptive field structure of cortical inhibitory neurons revealed by two-photon imaging guided recording. J Neurosci 2009;29:10520–10532. [PubMed: 19710305]
25. Liu BH, et al. Intervening inhibition underlies simple-cell receptive field structure in visual cortex. Nat Neurosci 2010;13:89–96. [PubMed: 19946318]
26. Smith PH, Populin LC. Fundamental differences between the thalamocortical recipient layers of the cat auditory and visual cortices. J Comp Neurol 2001;436:508–519. [PubMed: 11447593]
27. Richardson RJ, Blundon JA, Bayazitov IT, Zakharenko SS. Connectivity patterns revealed by mapping of active inputs on dendrites of thalamorecipient neurons in the auditory cortex. J Neurosci 2009;29:6406–17. [PubMed: 19458212]
28. Borg-Graham LJ, Monier C, Frégnac Y. Visual input evokes transient and strong shunting inhibition in visual cortical neurons. Nature 1998;393:369–373. [PubMed: 9620800]
29. Anderson JS, Carandini M, Ferster D. Orientation tuning of input conductance, excitation, and inhibition in cat primary visual cortex. J Neurophysiol 2000;84:909–926. [PubMed: 10938316]
30. Somers DC, Nelson SB, Sur M. An emergent model of orientation selectivity in cat visual cortical simple cells. J Neurosci 1995;15:5448–5465. [PubMed: 7643194]

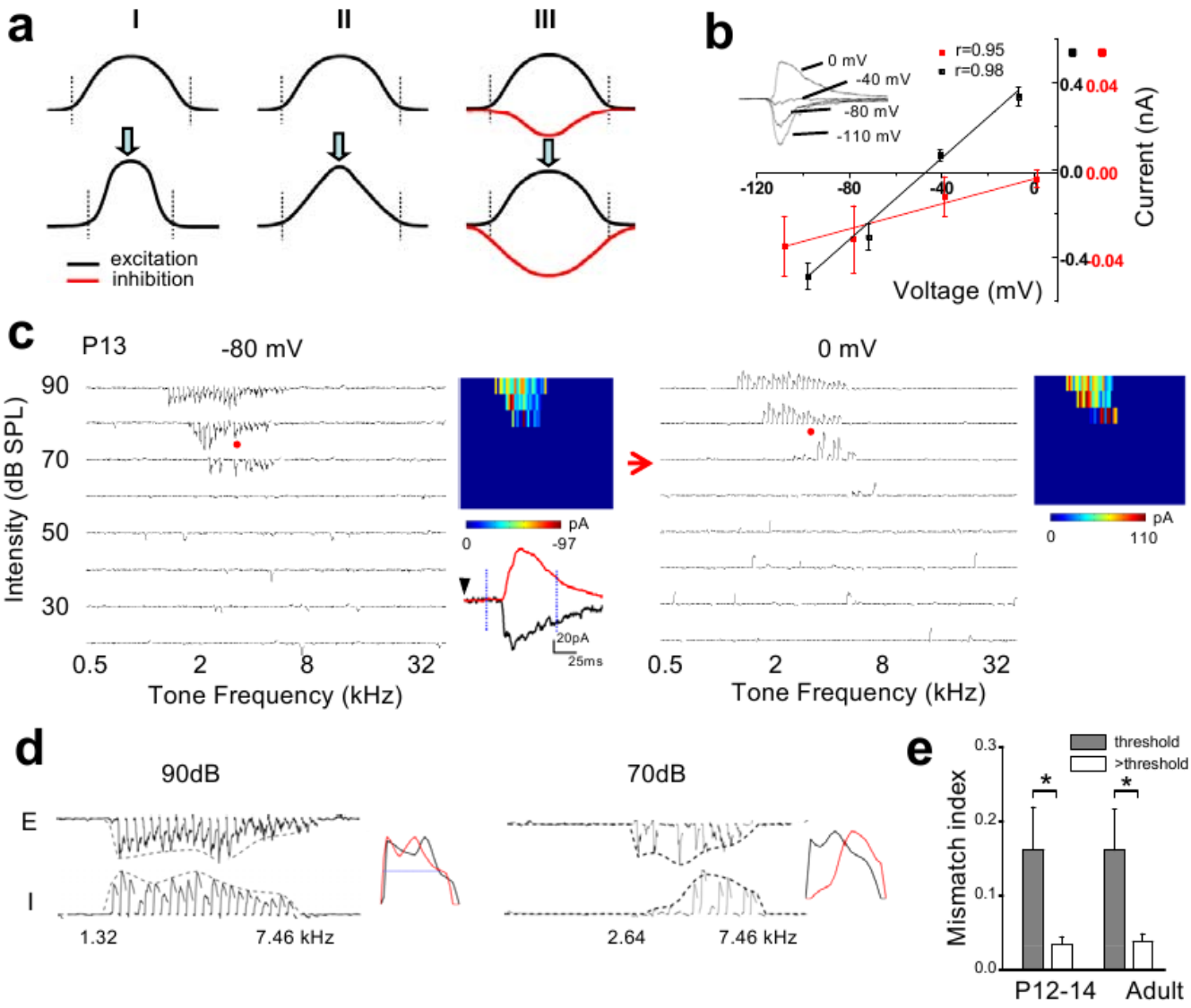

Figure 1. The synaptic TRFs shortly after the hearing onset

a, Three synaptic models for the functional refinement of sensory spike RFs (reduction in the size of RFs). Curves represent tuning profiles of excitation (black) and inhibition (red) along a sensory space. A pair of dotted vertical lines indicate the total responding range of excitatory inputs. I, pruning of peripheral excitatory inputs (i.e. reduced total responding range). II, adjustment of input strengths without pruning of inputs. III, broadening and strengthening of cortical inhibition. **b**, I-V curves for a recorded A1 neuron. Inset, average traces of synaptic currents (five repeats) of the neuron evoked by a noise stimulus. Average amplitude was measured within the 1–2ms (red) and 21–22ms (black) windows after the onset of the average synaptic response recorded at -80 mV. Correlation coefficient (*r*) is shown. **c**, TRFs of excitatory and inhibitory inputs for an example P13 neuron. Arrays of traces depict the excitatory (-80mV) and inhibitory (0mV) currents evoked by individual tone stimuli at various frequencies and intensities. Red arrow marks the intensity threshold. Color map depicts the peak amplitudes of tone-evoked synaptic currents within the TRF. The example excitatory (black) and inhibitory (red) responses evoked by the same tone (indicated by red dots) were enlarged. Dotted vertical lines mark the 75-ms window for plotting individual small traces in

the array. **d**, Frequency tuning curves of excitatory (E) and inhibitory (I) inputs to the same cell as in **b** at two intensities: the threshold (70dB) and 20 dB above the threshold (90dB). The starting and ending responding frequencies for the inhibitory tuning were marked. Right, the tuning curves are normalized and superimposed (E, black, reversed in polarity). Blue line indicates the half-peak level. **e**, Mismatch indices at threshold intensity (grey) and intensity of 20dB above threshold (white). For two P12–14 cells exhibiting an intensity threshold of 80 dB SPL, MMI was derived at 10dB above the threshold. *: $p < 0.005$, paired *t*-test, $n = 8, 6$ for P12–14 and adult, respectively. Error bar = s.d.

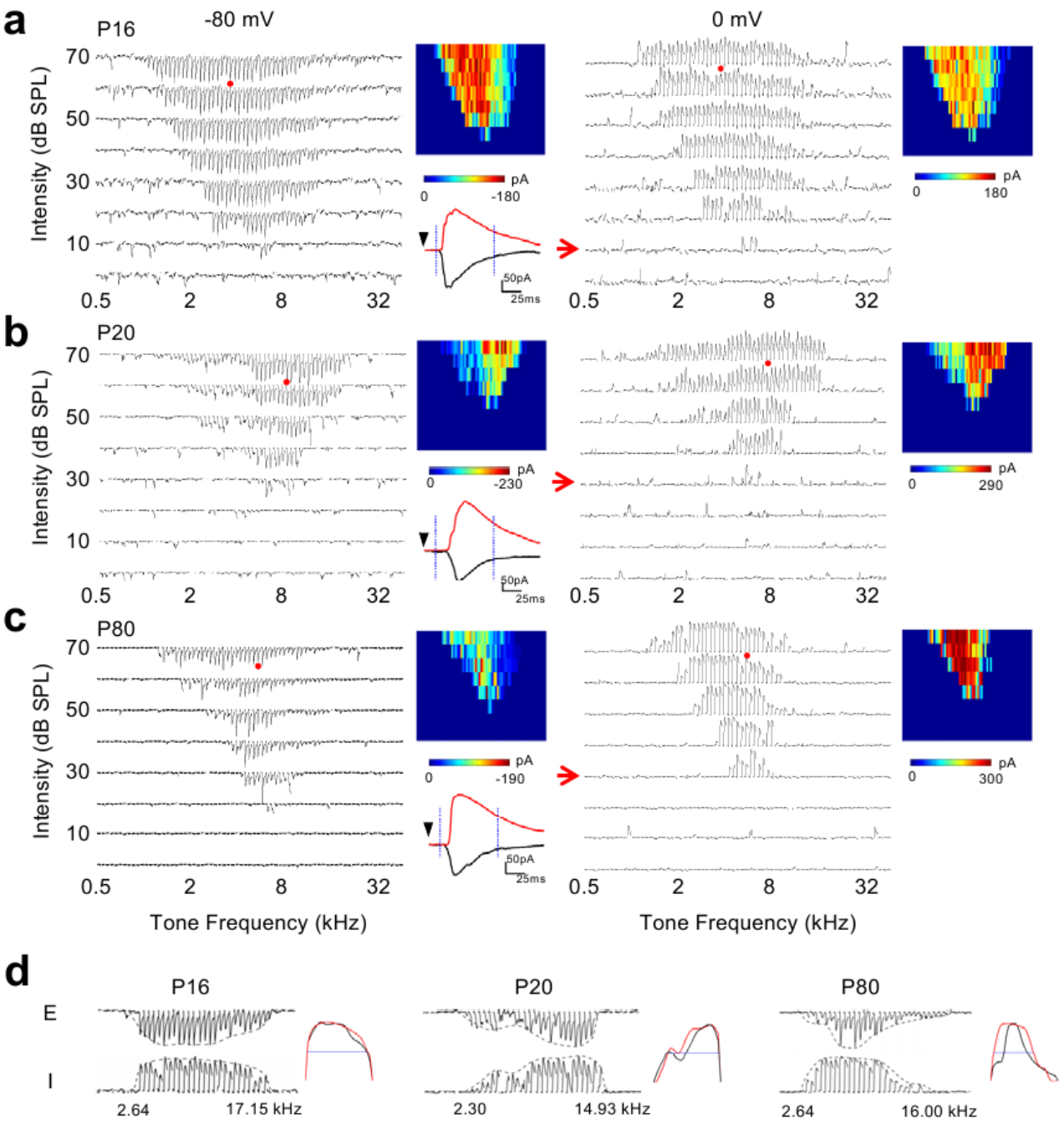

Figure 2. Synaptic TRFs at later developmental stages

a-c, Synaptic TRFs of example neurons at P16 (**a**), P20 (**b**) and P80 (**c**) respectively. **d**, Frequency tuning curves of excitatory and inhibitory inputs at the intensity of 20dB above threshold for cells shown in **a-c**. Presentation is the same as in Fig. 1.

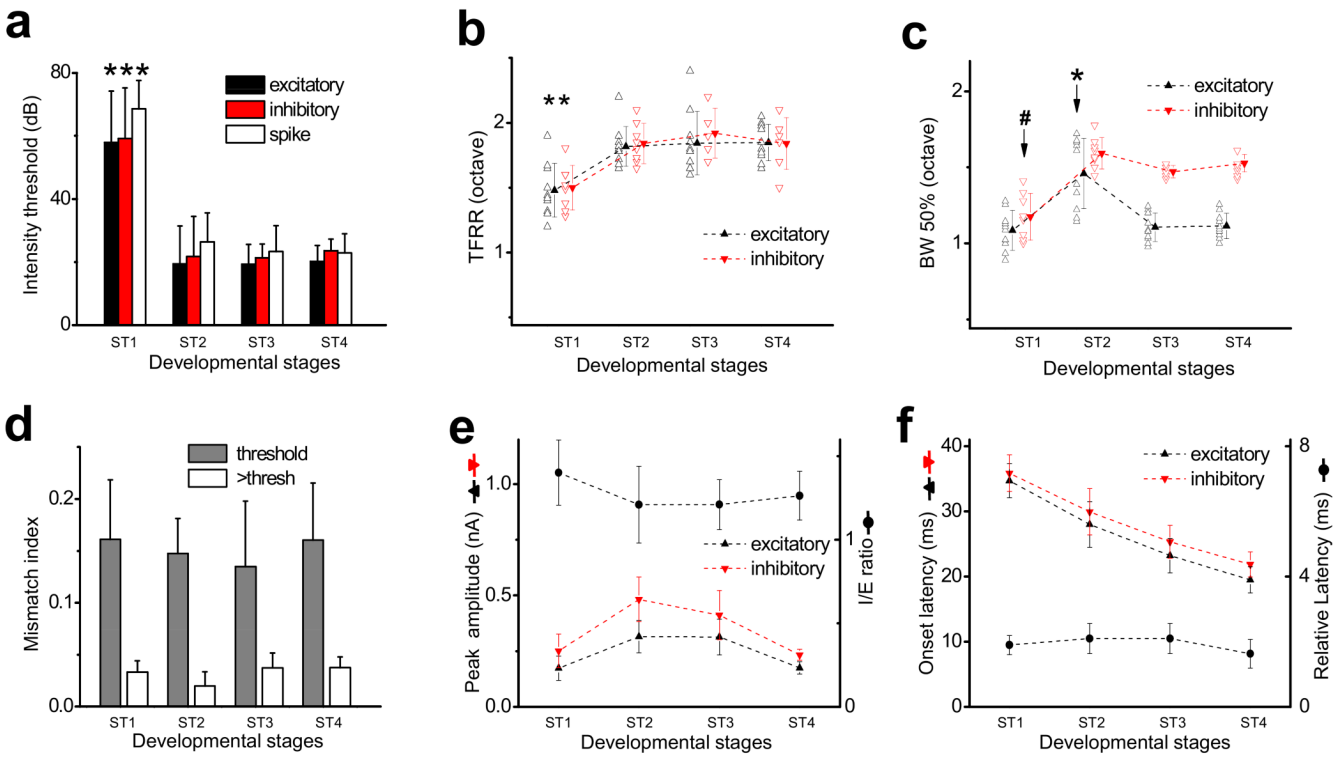

Figure 3. Developmental changes in spectral and temporal patterns of excitatory and inhibitory inputs

a, Average intensity threshold of excitatory, inhibitory and spike TRFs. ST1, P12-P14; ST2, P15-P18; ST3, P19-P25; ST4, ≥P80. *, significantly higher, $p < 0.001$, ANOVA *with post hoc* test, $n = 10, 10, 10, 10$ for excitatory, 8, 8, 5, 6 for inhibitory and 7, 11, 6, 14 for spike TRFs (by cell-attached recordings). **b**, Total frequency responding range (TFRR) of excitatory and inhibitory inputs at 10dB above intensity threshold. Data were from the same recordings as in **a**. Solid symbols are average values, and are connected with dotted lines for easier comparisons between neighbouring groups (the same for **c,e, and f**). *, significantly lower, $p < 0.05$, ANOVA with *post hoc*. **c**, Half-peak bandwidths (BW50%) of the tuning curves in **b**. *, difference in excitation; #, difference in inhibition; $p < 0.001$, ANOVA with *post hoc*. **d**, Mismatch indices at threshold intensity (grey) and 20dB above threshold (white) at different stages ($n = 8, 8, 5, 6$). For 20dB above threshold, ST2 is significantly lower than ST3 and ST4 ($p < 0.05$, ANOVA *with post hoc*). For each stage, MMI at threshold is significantly higher than at 20dB above threshold ($p < 0.005$, paired t-test). **e**, The average peak amplitudes of evoked inhibitory and excitatory currents from the same recordings as in **a**. The peak amplitude was determined by averaging five responses around the best frequency at the highest intensity tested. The I/E ratio was first calculated for individual cells with both excitatory and inhibitory TRFs recorded, and then averaged (circle, $n = 8, 8, 5, 6$, respectively). **f**, The onset latencies of synaptic responses, and the relative delay of inhibition. All error bars = s.d.

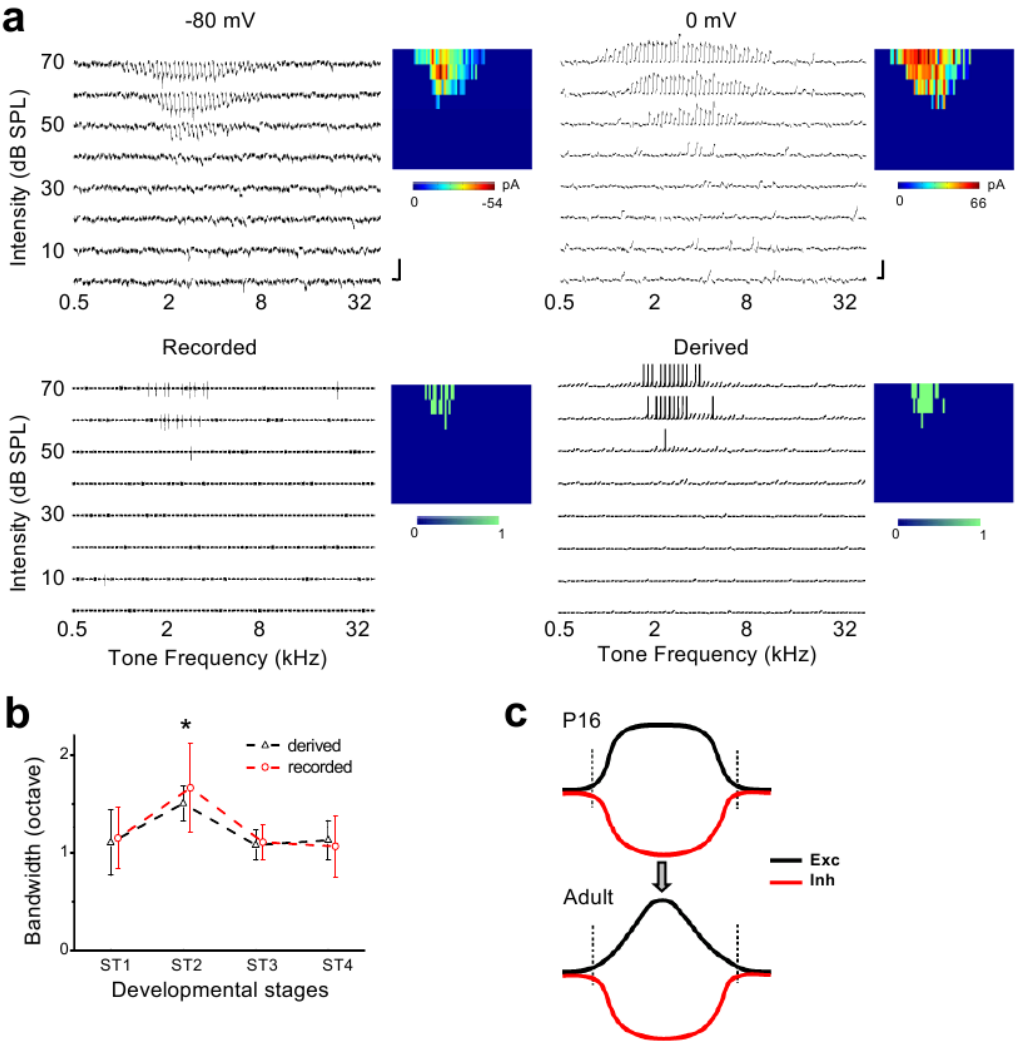

Figure 4. Synaptic mechanisms underlying the developmental refinement of spike TRFs in A1

a, An example cell with cell-attached recording followed by whole-cell recording. Top panels, the excitatory (-80mV) and inhibitory (0mV) TRFs of the cell. Scale: 50 pA and 100ms. Bottom left, the recorded spike TRF. Bottom right, the TRF of derived membrane potential and spike responses. Color maps represent the peak amplitudes of synaptic inputs (top), and number of spikes evoked (bottom). **b**, Bandwidths of spike TRFs derived and recorded from cells at different stages. Bandwidth was measured at 10dB above threshold. The value at ST2 is significantly higher (p = 0.1, 0.024, 0.014 between pairs of ST2-ST1, ST2-ST3 and ST2-ST4 respectively for recorded TRFs, n = 7, 11, 6, 14; p = 0.004, 0.016, 0.015 for derived TRFs, n = 8, 8, 5, 6, ANOVA *with post hoc*). Error bars = s.d. **c**, A developmental model. The excitatory (Exc) tuning profile is developmentally sharpened while the inhibitory (Inh) tuning remains relatively stable. Vertical lines mark the total range of inputs.